Development of Optimal PI Controllers for a Grid-Tied Photovoltaic Inverter

Ali Arzani[1], *Student Member, IEEE*, Paranietharan Arunagirinathan[1], *Student Member, IEEE*, and Ganesh Kumar Venayagamoorthy[1,2], *Senior Member, IEEE*
[1]Real-Time Power and Intelligent Systems Laboratory
Holcombe Department of Electrical and Computer Engineering, Clemson University, Clemson, SC 29634, USA
[2]Escom Centre of Excellence in HVDC Engineering, University of KwaZulu-Natal, Durban, South Africa
aarzani@g.clemson.edu, parunag@g.clemson.edu, and gkumar@ieee.org

***Abstract*—Power electronic interfaces (PEIs) play a significant role in integrating distributed energy sources (DER) into the electric power grid. In fact, as solution to grid integration of photovoltaic arrays, voltage source inverters (VSI) are widely utilized as the PEI entity. The VSI is controlled by a set of proportional-integral (PI) controllers, which require optimal tuning in order to guarantee smooth operation of PV-system especially when exposed to severe meteorological conditions e.g. sudden cloud covers. Hence, developing a practical robust tuning method for optimizing the PV-inverter set of controllers i.e. the DC-link voltage controller, the reactive power controller, and the decoupled current controller becomes of paramount importance. This paper employs a particle swarm optimization (PSO) approach to optimally tune these controllers based on online operation performance of the PV-system. The PSO approach is integrated into a real-time digital simulator (RTDS) for searching the inverter PI controllers parameters. The simulation results conclude the superiority of this approach in comparison to conventional inverter PI controller tuning methods; enhancing the PV-system transient and steady-state step-response over a wide operating range of irradiance.**

I. Introduction

DISTRIBUTED energy systems (DES) do not have fixed energy sources; sun irradiance, wind speed, and water-flows change during a day. Sophisticated grid interfaces are desired for these sources to enable non-fluctuating, reliable power to customers. The source of the DESs is mostly in DC form, as an example PV-arrays provide dc-voltage at their output. Thus, power electronic based inverters are required, enabling DC to grid-compatible AC conversion and vice-versa for grid interfacing. During the last two decades, converter technology has improved rapidly due to two main factors: firstly, as performance of power electronics semiconductor switches is improving from time to time, the trend to replace older technology with the newer improved ones with higher power handling capability and faster switching rates becomes of paramount importance [1]. Secondly, real-time computer/embedded controllers have made it possible to implement advanced control algorithms [2].

Knowing that all power electronic inverters exhibit a nonlinear behavior, various control laws can be uniquely designated and implemented based on the inverter type. Sliding-mode control [3] and conventional PI control methods [4] are applied for switched-model type inverters, while both linear and various nonlinear control methods can be applied to averaged-model type inverters. Thus, it can be deduced that the behavior of power electronic converter-based systems is highly dependent on its control structure performance. The more optimal the PI controllers are, the better PEI dynamic behavior will be during meteorological changes e.g. variations in irradiance in a PV-system or grid-side faults. As a result, an efficient and practical optimization method must be applied in order to achieve the most suitable system dynamic responses.

Particle swarm optimization [5], a computational intelligence approach, has been used by researchers for optimum design of PI/PID controllers of dynamic systems in multidisciplinary sciences. Gaing has utilized this optimization method to self-tune the PID controller in an AVR system, due to PSO capability in reaching an efficient solution in shorter computation time with better convergence characteristic in comparison to using GA for the same purpose [6]. Qiao *et al.* have reported that trial-and-error based optimal tuning for PI controllers of inverter-interfaced DFIG wind turbines is a cumbersome task and very hard due to complexity of back-to-back converters; so they have reached optimal solutions and consequently improved system performance over a wide range of operating points by applying PSO method [7]. Chung *et al.* have also opted for PSO method over manual tuning for the same reason as of [7] in operating microgrids [8]. Al-Saedi *et al.* investigate PSO in a three-phase grid-connected PV-system [9], however, their optimal solution is only for the four PV-inverter current controller parameters. This is because they have not optimized the four initial parameters of the DC-link voltage controller and reactive power controller (in case of PV-STATCOM operation of PV-inverter, the reactive power controller is also part of the VSI control structure).

This work is supported in part by US National Science Foundation (NSF) under grants #1312260 and #1308192, and the Duke Energy Distinguished Professor Endowment Fund. Any opinions, findings, and conclusions or recommendations expressed in this material are those of the author(s) and do not necessarily reflect the views of NSF and Duke Energy.

978-1-4799-7560-0/15 $31.00 © 2015 IEEE
DOI 10.1109/SSCI.2015.182

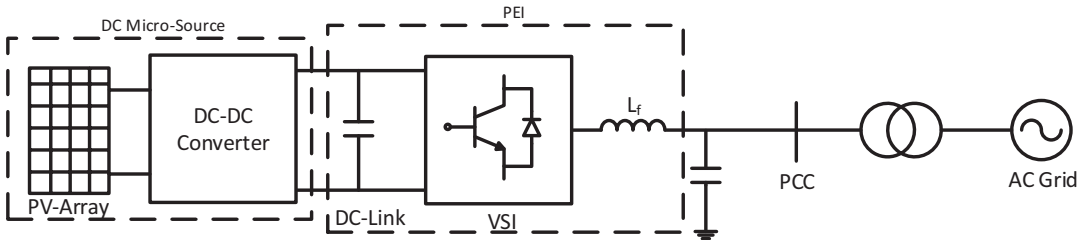

Fig. 1. Three phase PV-system model in RSCAD

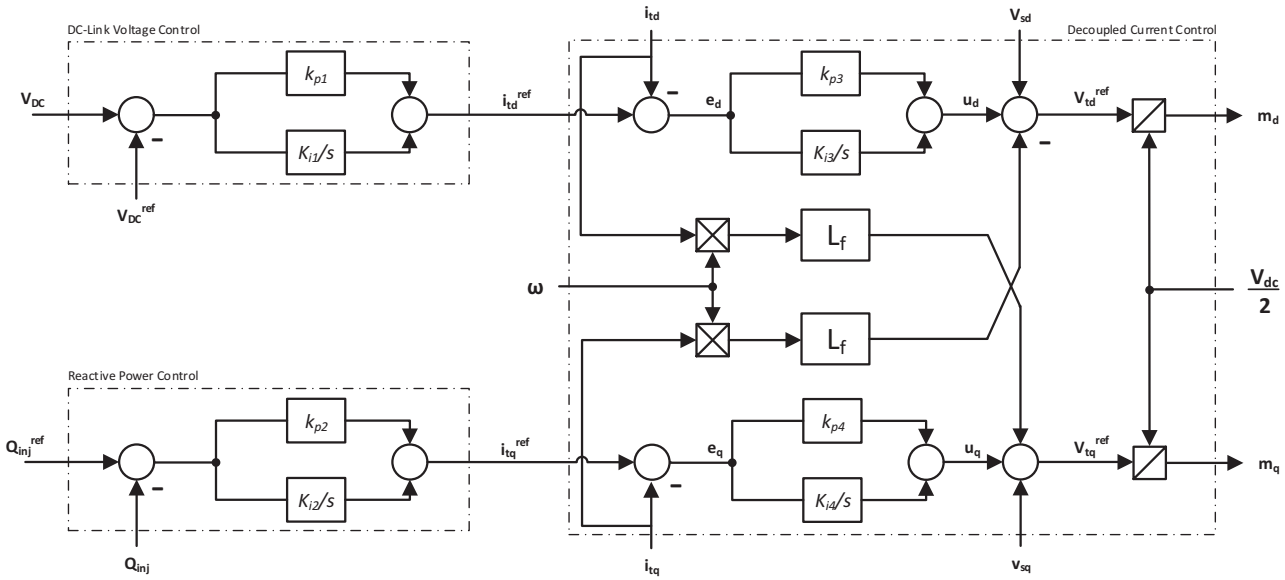

Fig. 2. PV-VSI control structure in $dq-$reference frame

In this paper, the PSO algorithm developed in MATLAB, has been integrated into a real-time digital simulator (RTDS) simulating a PV-system tied to a grid. The RTDS software (RSCAD) model interacts with the MATLAB code to arrive at optimal PI controller parameters for the PV-inverter. It is utilized to find all eight optimal parameters of the PV-inverter controllers using online operational performance. Three separate time-domain fitness functions have been defined in order to evaluate the performance of the PI controllers. The presented approach is an efficient and practical approach for on-site based tuning of PV-inverter controllers, to perform optimally over a wider range of operating irradiance conditions.

II. PV-system Model and Control

The PV-system studied and further developed in RSCAD comprises of a $53.55\,\mathrm{kW}$ PV-array connected to an infinite bus system grid through its PEIs and a $208\,\mathrm{V}-11\,\mathrm{kV}$, $Y0/Y0$ transformer as shown in Fig. 1. The PEIs are a DC-DC buck converter providing the maximum power and voltage of PV-array at each weather conditions as input to a two-level VSI. A passive low-pass filter is further installed at the output terminals of the inverter in order to eliminate the high-frequency switching harmonics in output current waveform.

The switch-model VSI and its associated control structure comprising of PI Controllers have been implemented based on $dq-$reference frame theory in RSCAD; this has been illustrated in Fig. 2. For a switch-model inverter as the circuit is switched at a high frequency i.e. in the realm of kHz, in order for the software to capture the complete circuit behavior by simulation, the minimum software solution time-step becomes paramount. This simulation time-step is small enough in RSCAD ($2\,\mu\mathrm{s}$) to capture complete performance of inverters at high switching frequencies up to $500\,\mathrm{kHz}$.

The two-level VSI as its circuit diagram for mathematical modeling is depicted in Fig. 3, controls power flow to the grid by utilizing the current control SPWM technique. The goal is to regulate the current output of the inverter to track a specified reference signal. It employs the following loop controls:

- Inner control loop i.e. decoupled current control
- Outer control loop i.e. DC-link voltage regulator
- Additional outer control loop for reactive power setting

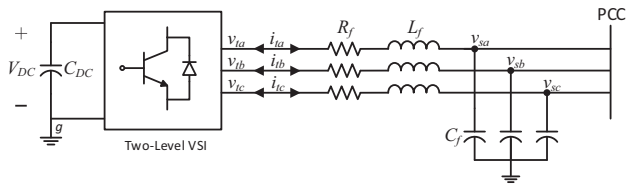

Fig. 3. Circuit diagram for mathematical description

The implemented closed-loop current control mechanism decouples the VSI dynamics from those of the grid; and controls the active and reactive currents, while the dc-link voltage control scheme regulates the dc link voltage to a reference value [10]. The $d-axis$ current regulates active power and the $q-axis$ current regulates reactive-power, for the reason that $V_{qs} \approx 0$ in synchronous reference frame.

$$P = \frac{3}{2}(V_{ds}^e I_{ds}^e + V_{qs}^e I_{qs}^e) \approx \frac{3}{2} V_{ds}^e I_{ds}^e \tag{1}$$

$$Q = \frac{3}{2}(V_{ds}^e I_{qs}^e - V_{qs}^e I_{ds}^e) \approx \frac{3}{2} V_{ds}^e I_{qs}^e \tag{2}$$

The DC-link voltage is maintained to a reference voltage value i.e. V_{DC}^{ref} by utilizing a first-order $PI-$controller. The commanded i_{td}^{ref} is fed to a $dq-$frame current controller (inner-control loop) in order to force i_{td} to track i_{td}^{ref}. Consequently, the control of i_{td} results injection of controllable non-zero active power to the grid while the PV-system operates close to unity power factor $(Q_s \approx 0)$.

The AC-side of the VSI can be mathematically modeled in the space-phasor domain as described by [10]:

$$\vec{v_t} + L_f \frac{d\vec{i_t}}{dt} + R_f \vec{i_t} + \vec{v_s} = 0 \tag{3}$$

The terminal voltage of the inverter is a controllable variable corresponding to the PWM modulation index $\vec{v_t} = \frac{v_{dc}}{2}\vec{m}$, where $\vec{m} = |\vec{m}| \angle m^\circ$ is the normalized modulating VSI switching signal. The current-controller has been modeled incisively based on feedback linearization, firstly introduced by Schauder and Mehta.

$$L_f \frac{di_{td}}{dt} = -R_f i_{td} + L_f \omega i_{tq} + m_d \frac{v_{dc}}{2} - v_{sd} \tag{4}$$

$$L_f \frac{di_{tq}}{dt} = -R_f i_{tq} - L_f \omega i_{td} + m_q \frac{v_{dc}}{2} - v_{sq} \tag{5}$$

Equations (4) and (5) indicate that the dynamics of i_{td} and i_{tq} are coupled and nonlinear. In order to decouple and linearize the dynamics around its equilibrium point for control applications (4) and (5) are rewritten accordingly:

$$m_d = \frac{2}{v_{dc}}(u_d - L_f \omega i_{tq} + v_{sd}) \tag{6}$$

$$m_q = \frac{2}{v_{dc}}(u_q + L_f \omega i_{td} + v_{sq}) \tag{7}$$

u_d and u_q are new inputs. By substituting (6) and (7) in (4) and (5), equations (8) and (9) are obtained, which provide two decoupled, linear first-order systems [10]:

$$L_f \frac{di_{td}}{dt} = -R_f i_{td} + u_d \tag{8}$$

$$L_f \frac{di_{tq}}{dt} = -R_f i_{tq} + u_q \tag{9}$$

Fig. 2 models the block diagram of the $dq-$reference frame current control scheme as part of the PV-system control structure, built based on equations (6) and (7). It is further observed that the control signals u_d and u_q have been formed accordingly in the current controller block-diagram:

$$u_d = (i_{tdref} - i_{td}) \cdot K_d(s) \tag{10}$$

$$u_q = (i_{tqref} - i_{tq}) \cdot K_q(s) \tag{11}$$

As it will be observed in section IV, the plant control parameters of (8) and (9) are not the same in value. However, both are first order systems in nature:

$$K_q(s) = K_d(s) = k_{px} + \frac{k_{ix}}{s} \tag{12}$$

Where time constant of the PI controllers should be small enough in order to provide a fast current control response [10].

III. PSO-Based PI−Controller Tunings

Tuning of all parameters of the four PV-inverter controllers has been accomplished utilizing PSO algorithm in a number of steps. Each PI controller has two parameters to tune in RSCAD, i.e. a proportional gain and a time constant. First, all eight parameters have been tuned by trial and error manually, by monitoring a number of factors, which define the dynamic response of the PV-inverter control waveforms. This has been a tedious task, in which proper procedures have been carried-out in order to achieve proper, but non-optimal tuning. Second, the parameter values from manual-tuning and their boundaries have been utilized effectively in order to initiate the PSO tuning process for the first four parameters of the outer control loop. The optimal values obtained from this step are used to find the most efficient and optimum solution for the inner control loop four parameters. The final result of this multi-step PSO-PI tuning is the optimal-tuning of all PV-inverter controllers, enhancing the PV-system transient and steady-state step-response of active power, reactive power, and DC-link voltage over a wide irradiance operating range.

A. Particle Swarm Optimization (PSO)

PSO is one of the swarm intelligence technologies inspired by the social behavior of flocks of birds and school of fish. This population based heuristic optimization method has been used for problems' optimization in various disciplines including electric power systems. The swarm space is defined with *N* particles and problem dimension *d*. For PI controller tuning, swarm is formed with one known initial solution and the rest randomly selected values and parameters within their boundaries. The lower limit and upper limit define their respective boundaries of each parameter to be tuned. Each particle is a solution to the problem, therefore the fitness evaluation (described in Section III-B) for each particle is calculated to discover their best position within the swarm space in every iteration. The fitness value calculated for each particle is called *pbest*. The minimum among the *pbest* values calculated is defined as the global best position, *gbest*. The particles change their position within the swarm space with iterations and move towards *gbest*. The *gbest* value is updated only if the minimum among the *pbest* values calculated is less than the present *gbest*. In order to change the position of each particle in every iteration, a velocity should be calculated. The velocity of n^{th} particle for i^{th} iteration is calculated using (13).

$$v_n^{i+1} = w.v_n^i + c_1 R_1 \left(pbest_n^i - x_n^i\right) + c_2 R_2 \left(gbest^i - x_n^i\right) \tag{13}$$

Where v_n is the velocity of particle n; w is an inertia weight usually in the range $0.4{-}1.2$; c_1 and c_2 are acceleration constants used to guide the particles to the *pbest* and *gbest* positions, respectively; and R_1 and R_2 are random numbers in the interval [0,1].

The position of each particle for the next iteration is calculated using the velocity calculated in (13) and its present position x_n^i accordingly:

$$x_n^{i+1} = x_n^i + v_n^{i+1} \tag{14}$$

Where x_n^i is the position of the n^{th} particle of i^{th} iteration and $x = [k_{p1}, T_{i1}, k_{p2}, T_{i2}, k_{p3}, T_{i3}, k_{p4}, T_{i4}]$.

Fig. 4 is the PSO tuning algorithm flowchart utilized; the termination criteria used is the maximum number of iterations.

B. Fitness Evaluation

The normalized active power (P), reactive power (Q) and DC voltage (V_{dc}) plot data collected for various step changes in solar irradiance are used to calculate the fitness values for each particle. The irradiance step changes made to capture plot data are given in Table I. The objective function calculates the area bounded by these plots. The fitness value of active power (P), reactive power (Q) and DC voltage (V_{dc}) are computed using (15), (16) and (17), respectively. Total fitness for the particle is calculated using equation (18).

TABLE I
IRRADIANCE STEP CHANGES

Step Change Case	Initial Irradiance (W/m^2)	Final Irradiance (W/m^2)
1	0	500
2	500	250
3	250	750

$$J_1 = \sum_{t=t_0}^{\frac{t_2-t_0}{\Delta t}} \left(\Delta P\left(t\right) - c_p\right)^2 \times \left(A \times \left(t - t_0\right) \times t\right) \tag{15}$$

$$J_2 = \sum_{t=t_0}^{\frac{t_2-t_0}{\Delta t}} \left(\Delta Q\left(t\right)\right)^2 \times \left(A \times \left(t - t_0\right) \times t\right) \tag{16}$$

$$J_3 = \sum_{t=t_0}^{\frac{t_2-t_0}{\Delta t}} \left(\Delta V_{dc}\left(t\right) - 1\right)^2 \times \left(A \times \left(t - t_0\right) \times t\right) \tag{17}$$

Where t is the simulation time in seconds, Δt is the simulation time step in seconds, t_0 is the instant of step change happens, t_2 is the simulation end time, A is a constant and ΔP, ΔQ, ΔV_{dc} are respectively change in active power, reactive power, DC voltage normalized. c_p is a constant used to shift the normalized active-power plot steady-state value down to zero on the $x - axis$. In this case c_p values used for different solar irradiance step changes 1, 2, and 3 listed in Table I are 0.478, 0.23, and 0.73, respectively.

The objective of the tuning is to minimize the time response of the active power, reactive power and DC voltage oscillations. The total fitness value J_T for m-step changes in solar irradiance is calculated as:

$$J_T = \sum_{k=1}^{m} (J_{1k} + J_{2k} + J_{3k}) \tag{18}$$

C. MATLAB-Based PSO and RSCAD Synchronization

The synchronization between MATLAB based PSO algorithm and RSCAD is achieved using transmission control protocol (TCP). The plot data collected for fitness evaluations and sending tuned PI controller parameters are achieved by running two different RSCAD scripts. The first script is used to control the TCP port opening to receive PSO tuned PI controller parameters from MATLAB. The second script is written to do the irradiance step changes and to save the plots for fitness calculation. This is achieved by running the RSCAD and MATLAB software on the same computer. Hence, plots saved to the computer storage space are read by MATLAB code and the fitness values are computed. This synchronization process has been elaborated in Fig. 5.

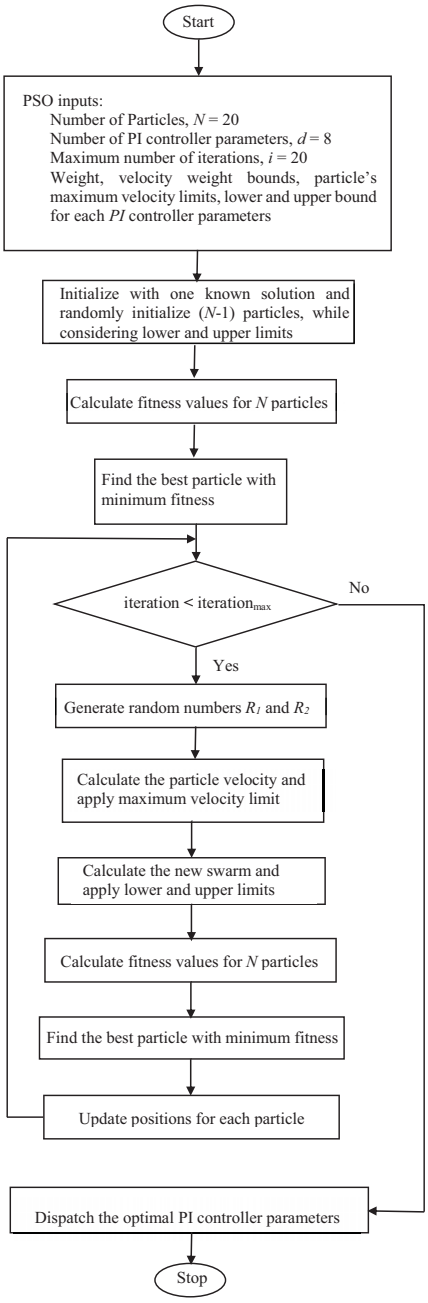

Fig. 4. The PSO algorithm flowchart

IV. Simulation Results

The PI controllers of all three inner and outer control loops of the PV-inverter described in Section II are initially tuned non-optimally with trial-and-error procedure for the complete operating range of the PV-array irradiance i.e. complete cloud cover $S = 0(W/m^2)$ to full sun $S = 1000(W/m^2)$, when the temperature of the PV-array is considered constant at $T_{ref} = 25\,^{\circ}\mathrm{C}$. The normalized active power injected to the grid P, reactive power injected Q, and the PV-inverter DC-link voltage V_{dc} have been shown for three test cases i.e. irradiance step-changes of 0 to 500, 500 to 250, and 250 to $S = 750(W/m^2)$, respectively. The step-response to each of the aforementioned irradiance cases are depicted in Figs. 6, 7, and 8, respectively. The PI and PSO-PI controllers upper and lower limits for obtaining these waveforms were pre-defined to the values given in Table II during the simulations.

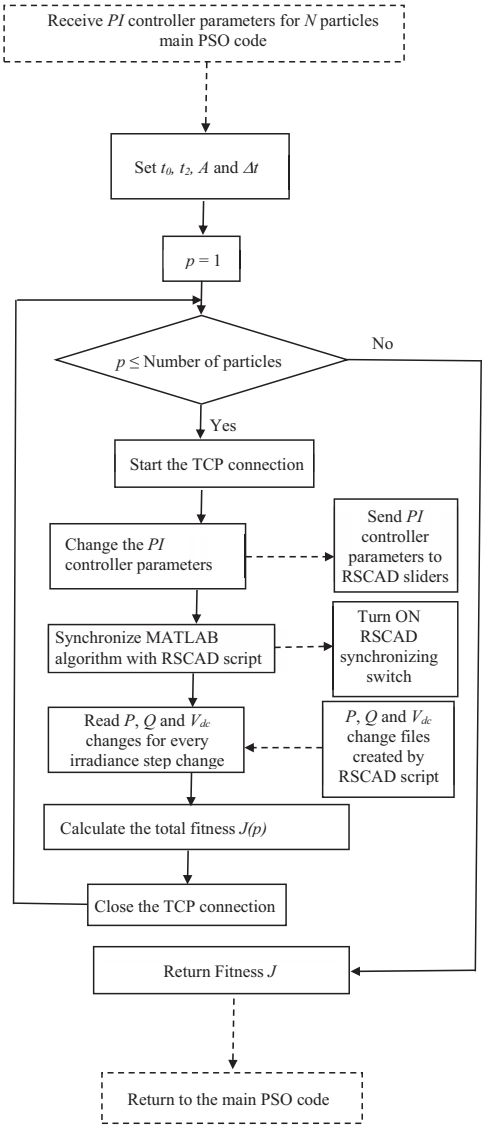

Fig. 5. Subroutine for RSCAD-MATLAB interface and total fitness function calculation

The optimal tuning parameters for the four PI controllers have resulted from the final PSO simulation and listed in Table III. With the final fine tuning parameters as input to the PV-inverter controllers, the 2^{nd} PSO-PI Tuning waveforms (dynamic responses to step-change in irradiance when all eight parameters have been optimally tuned) have been obtained. The final optimum tuning of eight parameters have been achieved according to the steps explained in Section III.

TABLE II
RANGE OF FOUR PV-INVERTER CONTROLLER PARAMETERS

VSI Controller Parameters		Minimum Value	Maximum Value
Outer Control Loops	k_{p_1}	0.002	5
	T_{i_1}	0.0001	0.5
	k_{p_2}	0.01	3
	T_{i_2}	0.0001	0.5
Inner Control Loop	k_{p_3}	0.1	15
	T_{i_3}	0.001	0.5
	k_{p_4}	0.1	10
	T_{i_4}	0.001	0.5

TABLE III
RESULTS OF PV-INVERTER CONTROLLERS TUNING METHODS (A) TRIAL & ERROR, (B) PSO-PI OUTER LOOP, (C) PSO-PI INNER LOOP

VSI Controller Parameters	Initial PI Tuning	1st PSO−PI Tuning	2nd PSO−PI Tuning
k_{p_1}	2	3.5467	3.5467
T_{i_1}	0.02	0.0014	0.0014
k_{p_2}	1	1.9389	1.9389
T_{i_2}	0.05	0.1846	0.1846
k_{p_3}	10	10	9.0243
T_{i_3}	0.05	0.05	0.2975
k_{p_4}	3.4	3.4	3.8011
T_{i_4}	0.05	0.05	0.0650

TABLE IV
PV-SYSTEM STEP-RESPONSE PERFORMANCE SPECIFICATION FOR THREE TYPES OF PV-VSI CONTROLLERS

Irradiance Step Change	Type of Controller	*Active Power (pu)* P_{peak}	P_{ss}	$M_p(\%)$	$t_s(sec)$	*DC-Voltage (pu)* $V_{DC_{peak}}$	$V_{DC_{ss}}$	$M_p(\%)$	$t_s(sec)$
$0 \rightarrow 500W/m^2$									
	Manual	0.7880	0.4778	64.92	2.988	1.0591	1.0001	5.9	3.6128
	1st PSO-PI	0.6487	0.4779	35.74	0.368	1.0132	1.0000	1.32	0.3664
	2nd PSO-PI	0.6489	0.4782	35.7	0.368	1.0132	1.0000	1.32	0.3664
$500 \rightarrow 250W/m^2$									
	Manual	0.0735	0.2295	−67.97	0.3248	0.9685	1.0000	−3.15	1.9600
	1st PSO-PI	0.0961	0.2295	−58.13	0.1200	0.9919	1.0000	−0.81	0.1984
	2nd PSO-PI	0.0932	0.2295	−59.39	0.1184	0.9917	1.0000	−0.83	0.1984
$250 \rightarrow 750W/m^2$									
	Manual	1.0442	0.7331	42.44	3.7984	1.0617	1.0000	6.18	8.3168
	1st PSO-PI	0.9721	0.7319	32.82	0.5248	1.0165	1.0000	1.65	0.4144
	2nd PSO-PI	0.9725	0.7313	32.98	0.5200	1.0165	1.0000	1.65	0.4112

It is observed that zero steady-state error $(e_{ss} = 0)$ has been achieved in all three types of designed PV-inverter controllers, verifying the proper tuning in all types. However, in order to define the optimum controller type, further time-domain dynamic analysis of the PEI needs to be carried out. The results of this analysis are given in Table IV, where the performance criteria for calculating the settling time for P and V_{dc} are $\pm 5\%$ and $\pm 0.5\%$, respectively.

It can be deduced from analyzing the data in Table IV and comparing the relative 2^{nd} PSO-PI tuning waveforms with the waveforms obtained from manual tuning in Figs. 6-8 that:

Active Power Injection: In all step-changes both overshoot and settling time have decreased significantly.

Reactive Power Injection: It is close to zero and oscillations are being damped faster. Note that there is no Q injection towards the AC grid, since the reference to track by the reactive power controller is set to zero as the system is operated during daytime. The very small amount of MVAr that is injected from the AC side is due to the transformer. However, its transient response is analyzed here.

DC-Link Voltage: substantial improvements in both overshoot and settling time. The reference-point $1pu$ is maintained in an accurate and rapid manner.

Further, when analyzing the active power injection in test case (2), it is observed that when the 2^{nd} PSO-PI tuning has been performed (2^{nd} controller type), the overall steady-state response has further improved in comparison to 1^{st} PSO-PI tuning (1^{st} controller type). Thus, it can be concluded from the time-response analysis and figures that the optimum tuning has been achieved in 2^{nd} PSO-PI tuning implementation, where all four controller parameters are tuned using PSO in multi-steps.

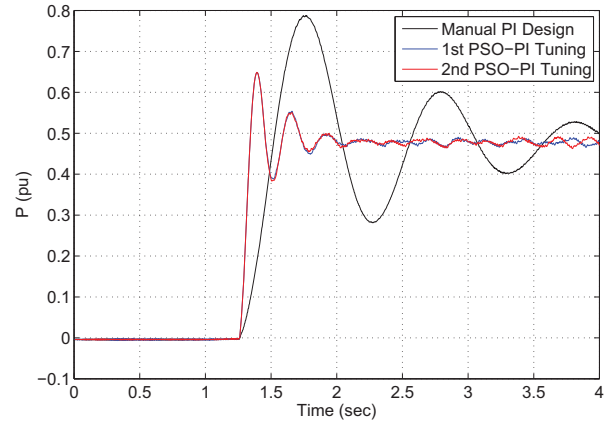

(a)

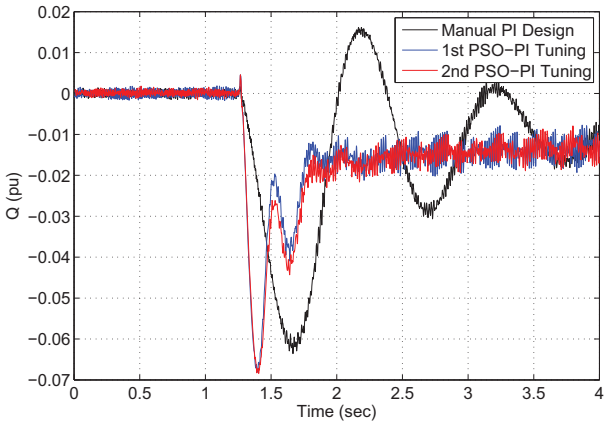

(b)

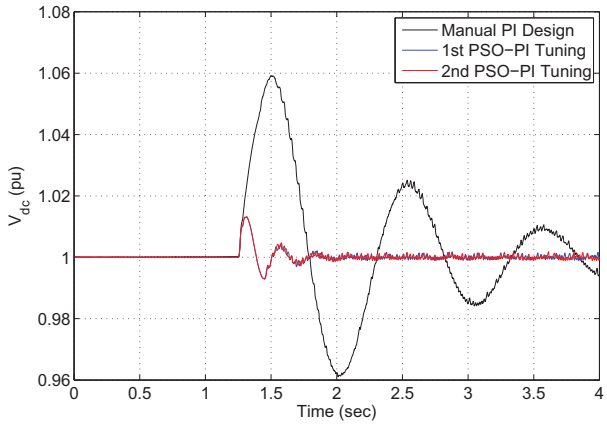

(c)

Fig. 6. PV-inverter dynamic responses with respect to irradiance step-change from $S = 0W/m^2$ to $S = 500W/m^2$ (a) active power, (b) reactive power, (c) dc-link voltage.

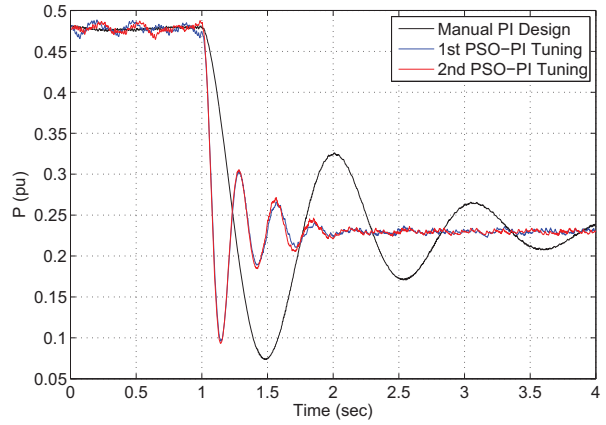

(a)

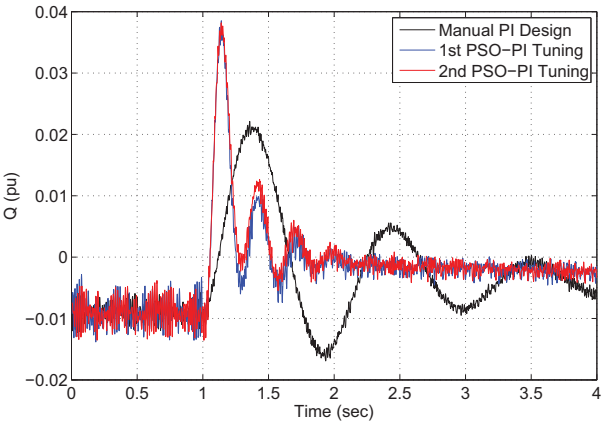

(b)

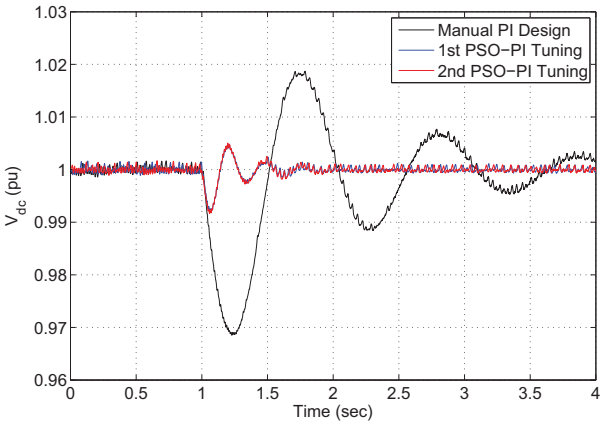

(c)

Fig. 7. PV-inverter dynamic responses with respect to irradiance step-change from $S = 500W/m^2$ to $S = 250W/m^2$ (a) active power, (b) reactive power, (c) dc-link voltage.

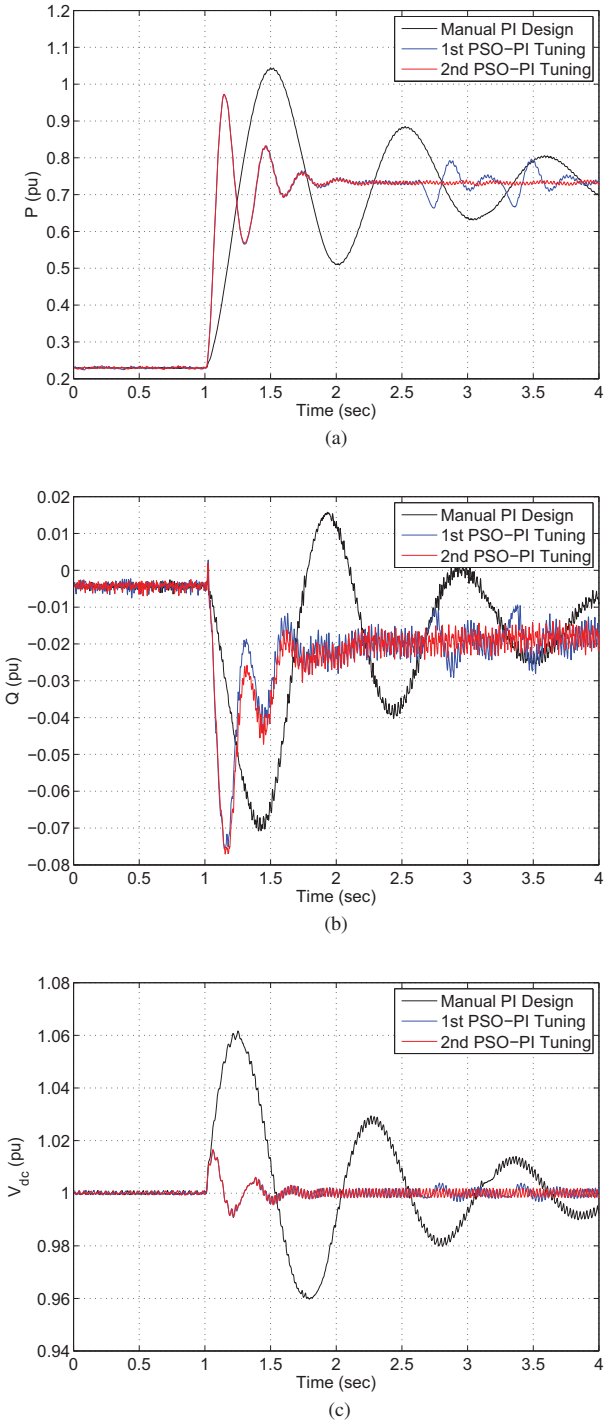

Fig. 8. PV-inverter dynamic responses with respect to irradiance step-change from $S = 250W/m^2$ to $S = 750W/m^2$ (a) active power, (b) reactive power, (c) dc-link voltage.

V. Conclusion

Voltage source inverters are extensively utilized as the interface between DC renewable energy sources and the AC grid nowadays. These inverters have emerged as one of the most indispensable components in smart grid operations. Thus, optimal controllers are of paramount importance. Due to complexity of switch-mode PV-inverters, optimal tuning of the PV-VSI can become a tedious task. Thus, particle swarm optimization algorithm to optimally tune these controllers during real-time operation of the PV-system has been investigated in this study. This approach has been implemented on a real-time simulation model of a PV grid-tied system. The simulation results illustrate the superiority of this optimal controller development approach in comparison to conventional inverter PI controller tuning methods. This is evident as the transient response of the waveforms have improved with optimal tuning of the PV-inverter controllers; enhancing the PV-system dynamic response over a wide irradiance operating range.

References

[1] A. Arzani, "Design and Control of a Novel Dynamic Hybrid VAR Compensator", M.Sc. Thesis, Royal Institute of Technology (KTH), XR-EE-EME 2010:007, Stockholm, Sweden, November 2010.

[2] J.M. Carrasco *et al.*, "Power-Electronic Systems for the Grid Integration of Renewable Energy Sources: A Survey", *IEEE Transactions on Industrial Electronics*, vol. 53, no. 4, 2006.

[3] S. Bacha, I. Munteanu, and A.I. Bratcu, *Power Electronic Converters Modeling and Control*, Springer Press, 2014.

[4] A. Keyhani, M.N. Marwali, and M. Dai, *Integration of Green and Renewable Energy in Electric Power Systems*, Wiley Press, 2009.

[5] Y. Del Valle, G.K. Venayagamoorthy, S. Mohagheghi, J.C. Hernandez, and R.G. Harley, "Particle Swarm Optimization: Basic Concepts, Variants and Applications in Power Systems", *IEEE Transactions on Evolutionary Computation*, vol. 12, no. 2, pp. 171-195, 2008.

[6] Z.L. Gaing, "A Particle Swarm Optimization Approach for Optimum Design of PID Controller in AVR System", *IEEE Transactions on Energy Conversion*, vol. 19, no. 2, pp. 384-391, 2004.

[7] W. Qiao, G.K. Venayagamoorthy, and R.G. Harley, "Design of Optimal PI Controllers for Doubly Fed Induction Generators Driven by Wind Turbines Using Particle Swarm Optimization", in *Proc. International Joint Conf. on Neural Networks (IJCNN)*, July 2006.

[8] I.Y. Chung, W. Liu, D.A. Cartes, and K. Schoder, "Control Parameter Optimization for a Microgrid System Using Particle Swarm Optimization", in *Proc. IEEE International Conf. on Sustainable Energy Technologies (ICSET)*, 2008.

[9] W. Al-Saedi, S.W. Lachowicz, and D. Habibi, "An Optimal Current Control Strategy for a Three-Phase Grid-Connected Photovoltaic System Using Particle Swarm Optimization", in *Proc. Power Engineering and Automation Conf. (PEAM)*, 2011.

[10] A. Yazdani and P. Dash, "A Control Methodology and Characterization of Dynamics for a Photovoltaic (PV) System Interfaced With a Distribution Network", *IEEE Transactions on Power Delivery*, vol. 24, no. 3, pp. 1538-1555, July 2009.